CHROM. 23 553

Isotachophoretic separation of minor components from a matrix component in the case of strong electrolytes☆

Takeshi Hirokawa*, Akihiro Omori, Yasuro Yokota☆☆, Jian-Ying Hu and Yoshiyuki Kiso

Applied Physics and Chemistry, Faculty of Engineering, Hiroshima University, Kagamiyama 1, Higashi-Hiroshima 724 (Japan)

ABSTRACT

In order to clarify the cause of underestimation in the isotachophoretic analysis of minor components, the effect of the ratio of sample components on the separation efficiency was studied on the basis of computer simulation and the observation of the transient state of separation. It was confirmed for binary mixtures of strong electrolytes that the separation efficiency was almost unaffected by this ratio. On the other hand, when the number of sample components was more than two, the resolution time was no longer independent of the component ratio. However, if the total molar amount was kept constant, the dependence was not so serious and the resolution time was about double that for the equimolar mixture. The most important point in the analysis of the isotachopherogram of minor components was to avoid overloading of the sample solution, as the formation of a mixed zone of the matrix and a minor component is difficult to detect.

INTRODUCTION

One of the practical problems encountered in isotachophoretic analysis is the underestimation of minor components in a matrix component. The essential reason is sample overloading, *i.e.*, when the amount of electricity is insufficient for the separation of a sample, the sample zones would reach the detector before complete separation [1,2]. If the number of sample components is known and they are nearly equimolar, the unresolved zone is easily distinguished. However, in minor component analysis, a serious point is that the mixed zone between the minor component and the matrix is frequently overlooked, as the detector signals of the mixed zone resemble those of the steady-state zone of the matrix component, whatever detector is used. As a result, the separation tube tends to be overloaded to increase the zone length of the minor components. Therefore, it is natural that the minor components are sometimes underestimated. To avoid such underestimation, the zone length of the steps in isotachopherograms should be carefully checked by varying the amount of the sample injected.

In a previous paper [3], we clarified the cause of the delay in the resolution time of a two-component mixed zone by the addition of a third component (the composition effect on the separation efficiency). It was due to the change in the potential gradient of the binary mixed zone and the extent of the delay depended on both the molar amount and the mobility of the co-existing sample components. The present problem with minor component analysis is closely related to the composition effect.

In order to clarify how the separation efficiency of minor components is affected by the matrix com-

---

ponent, the separation process of six components was simulated by varying the ratio of the molar amounts. The separation processes of several actual samples were observed by the use of a 32-channel UV photometric array detector and an ultraviolet (UV) scanning detector [4]. The observed resolution time was compared with the simulated time to confirm the validity of the simulation. Practical aspects concerning the quantitative determination of minor components using zone lengths are also discussed.

THEORETICAL

Two-component mixture

Assume two monovalent strong ions, A and B. The absolute mobility of ion A (m_A) is larger than that of ion B (m_B). In the separation process, the two-component mixed zone AB is formed from the solution injected. The resolution time of the zone AB can be expressed as follows [5,6]:

$$t_{res,AB} = \frac{l_A}{E_A \overline{m}_A - E_{AB} \overline{m}_{B,AB}} \quad (1)$$

where l_A is the zone length of component A in a separation tube after the AB mixed zone is resolved (the steady state), E_A the potential gradient of zone A at the steady state, $\overline{m}_A$ the effective mobility of ion A in zone A, E_{AB} the potential gradient of the mixed zone AB and $\overline{m}_{B,AB}$ the effective mobility of ion B in the mixed zone.

A different expression for $t_{res,AB}$ is obtained on the assumption that the separation process follows the diagram reported by Brouwer and Postema [7]:

$$t_{res,AB} = \frac{l_B}{E_{AB} \overline{m}_{A,AB} - E_B \overline{m}_B} \quad (2)$$

where l_B is the zone length of component B at the steady state, $\overline{m}_{A,AB}$ the effective mobility of ion A in the mixed zone, E_B the potential gradient of zone B and $\overline{m}_B$ the effective mobility of ion B.

In a previous paper [3], we showed that the resolution time of a binary mixture, $t_{res,AB}(2)$, can be expressed by a simple equation reduced from eqn. 1, when the components are equimolar strong electrolytes. If the components are not equimolar, one can derive the following equation on the basis of similar assumption:

$$t_{res,AB}(2) = \frac{Fn_t}{i(N_R + 1)} (1 + m_Q/m_A) \frac{\overline{m}_A + N_R \overline{m}_B}{\overline{m}_A - \overline{m}_B} \quad (3)$$

$$N_R = n_B/n_A \quad (4)$$

$$n_t = n_A + n_B \quad (5)$$

where N_R is the ratio of the molar amount of components A and B (n_A and n_B), n_t the total amount, F the Faraday constant, i the migration current and m_Q the absolute mobility of counter ion as the pH buffer. The potential gradient of E_{AB} was expressed using E_A as follows:

$$E_{AB} = \frac{(1 + N_R)\overline{m}_A}{\overline{m}_A + N_R \overline{m}_B} \cdot E_A \quad (6)$$

With the ultimate conditions $n_A \gg n_B$ and $n_A \ll n_B$, the following expressions are obtained.

Case $n_A \gg n_B$. In this case N_R is very small and component A can be regarded as the matrix component, and eqn. 1 suggests that the resolution time reaches to a limiting value defined as follows:

$$t_{res,AB}(2) = \frac{Fn_t}{i} (1 + m_Q/m_A) \frac{\overline{m}_A}{\overline{m}_A - \overline{m}_B} \quad (7)$$

It is apparent from eqn. 6 that E_{AB} approaches the potential gradient of the matrix component A at the steady state:

$$E_{AB} \approx E_A \quad (8)$$

Case $n_A \ll n_B$. By reducing eqn. 2, one can obtain a different expression for $t_{res,AB}(2)$ as follows:

$$t_{res,AB}(2) = \frac{Fn_t}{i(1/N_R + 1)} (1 + m_Q/m_B) \frac{\overline{m}_A/N_R + \overline{m}_B}{\overline{m}_A - \overline{m}_B} \quad (9)$$

where t_B is the time-based zone length of zone A at the steady state. When N_R is larger than 1 and component B can be regarded as the matrix component, the limiting resolution time at $N_R = \infty$ can be expressed as follows:

$$t_{res,AB}(2) = \frac{Fn_t}{i} (1 + m_Q/m_B) \frac{\overline{m}_B}{\overline{m}_A - \overline{m}_B} \quad (10)$$

E_{AB} can be correlated with E_B as follows:

$$E_{AB} = \frac{\overline{m}_B(1 + N_R)}{\overline{m}_A + N_R\overline{m}_B} \cdot E_B \qquad (11)$$

It is apparent from eqn. 11 that E_{AB} approaches the potential gradient of the matrix component B at the steady state when N_R is very large:

$$E_{AB} \approx E_B \qquad (12)$$

It should be noted that the values of the resolution time under the extreme conditions $n_A \gg n_B$ and $n_A \ll n_B$ are almost equal when the total amount of the sample components is constant:

$$\frac{t_{res,AB}(2)_{N_R = \infty}}{t_{res,AB}(2)_{N_R = 0}} = \frac{m_B + m_Q}{m_A + m_Q} \approx 1 \qquad (13)$$

The resolution time of a binary mixture is almost insensitive to the sampling ratio, when the mobility difference is small and the components are monovalent ions. If one of the components is multivalent, there will be a distinct difference as its time-based zone length differs significantly from that of the monovalent ion. An example for actual samples will be shown later.

The potential gradient of the mixed zone is always between the two extreme values of E_A and E_B:

$$E_A < E_{AB} < E_B \qquad (14)$$

The validity of these equations will be discussed later in comparison with the separation process of actual samples.

Multi-component mixture

In this instance, the separation efficiency of the binary mixed zone of interest will be affected by the existence of the other components, as discussed for the equimolar mixture in a previous paper [3]. As the extent of the delay of the resolution time depends on the amount and the mobility of the coexisting ions, the resolution time of the mixed zone is no longer independent of the component ratio. However, provided that the total molar amount of the sample is kept constant, the change in the resolution time is not so serious, as shown later.

To confirm the above conclusion for the minor components, first the separation process of a binary mixture was studied in detail, varying the ratio of the component amounts. Then the effect of the component ratio on the resolution time of a four-component mixture was studied.

EXPERIMENTAL

The samples used were 4,5-dihydroxy-3-(*p*-sulphophenylazo)-2,7-naphthalenedisulphonic acid (SPADNS), monochloroacetic acid (MCA) and picric acid (PA). Except for MCA, these samples absorb visible and UV light. The sodium salt of SPADNS was purchased from Dojin (Kumamoto, Japan) in the purest form. The other chemicals were guaranteed-grade reagents obtained from Tokyo Kasei (Tokyo, Japan). Stock sample solutions were prepared by dissolving them in distilled water without further purification.

Mixtures of SPADNS and MCA (SM) and of MCA and PA (MP) were used for the observation of the characteristics of binary mixtures. The pairs were selected so as to contain UV-transparent MCA. This is very important in transient state analysis using a UV detector, as will be apparent in the observed isotachopherogram. The ratio of the sample components was varied in the range 100:1 to 1:100. The total amount of the mixture injected was 50 nmol for SM and 35 nmol for MP. The pH of these solutions was adjusted to 3.6 by adding β-alanine.

An array detection system constructed in our laboratory [8] was used to observe the separation process of these two-component mixtures. The array detector had 32 equidistant UV detectors along a 16-cm separation tube. A single cycle to acquire the UV signals, namely time resolution of the system, was 243.2 ms. Usually 5000–7000 data were acquired in a single run. In order to determine the boundary-detected time and the boundary velocity, the observed UV signals were differentiated with respect to time, and the positive and negative peaks of the differentiated signals were searched for. Linear equations describing the progression of the boundaries can be evaluated by the least-squares method on the basis of these numerical data. The resolution time can be obtained by solving simultaneous equations for the different boundaries.

A potential gradient profile for the binary mix-

ture MP was also measured by the use of a Shimad-zu (Kyoto, Japan) IP-2A isotachophoretic analyser. The ratio of sample amounts was MCA:PA = 10:1.

The four-component mixture used was a solution of SPADNS, MCA, PA and 2,3-dihydroxybenzoic acid (DBA), the SPADNS:MCA:PA:DBA ratio being varied from 1:1:1:1 to 10:1:1:1. The total amount of the sample injected was 100 nmol and the volume injected was 10 μl. A scanning UV photometric detector was used for the observation of the separation process. For scanning a linear head equipped with a UV lamp and a detector was driven by a computer-controlled stepping motor. The separation tube used was a fused-silica capillary (32 cm × 0.53 mm I.D. × 0.7 mm O.D.). The UV radiation from a deuterium lamp was passed through a UV glass filter (Toshiba Glass, Tokyo, Japan; Model D33S, λ_{max} = 330 nm). A single cycle to scan the 32-cm tube was 7.025 s and the number of data in a single scan was 5333. The resolution was 0.06 mm per data point, which was sufficient to trace the separation process accurately. For data acquisition, an NEC (Tokyo, Japan) PC9801VX microcomputer was used (CPU = 80286, coprocessor = 80287, clock 10 MHz). All experiments were carried out at 25°C.

The concentration of the leading electrolyte (hydrochloric acid) was 5 mM. The pH was adjusted to 3.6 by adding β-alanine. A 5 mM leading electrolyte was used in order to avoid the saturation of the UV detector owing to the high concentration of the sample in each zone. The migration current applied was 50 μA. The terminator was 10 mM caproic acid. Hydroxypropylcellulose (HPC, 0.2%) was added to the leading and terminating electrolytes to suppress electroendosmosis. The viscosity of a 2% aqueous solution is 1000–4000 cP at 20°C according to the specification. The sample solution was injected into the terminating electrolyte near the boundary between the leading and terminating electrolytes. The pH of the terminating electrolyte was also adjusted to 3.6 by adding β-alanine to ensure that the pH of the sample solution at the initial stage of migration was equal to the prepared value. The pH measurements were carried using a Horiba (Tokyo, Japan) Model F7ss expanded pH meter.

In the simulations of the transient state, the microcomputer used was an NEC PC-9801RA2 (CPU = 80386, coprocessor = 80387, clock 16 MHz). The physico-chemical constants used in the simulations are summarized in Table I. In our simulation program SIPSR [3,9,10], the effect of the ionic strength on the mobility and dissociation constants were corrected. However, in the correction the viscosity of pure water was used as that of electrolyte solution in the separation tube, although the electrolyte contained HPC and other chemicals. This may cause small errors in simulation.

RESULTS AND DISCUSSION

Two-component mixture

Table II shows the resolution time of the binary mixtures exactly simulated for several model anions using our computer program SIPSR [3,9,10]. Table II also summarizes the approximate values obtained by the use of eqn. 3. The mobility of ion A was 60 · 10^{-5} or 30 · 10^{-5} cm^2 V^{-1} s^{-1} and the mobility difference between ions A and B was in the range 1 · 10^{-5}–10 · 10^{-5} cm^2 V^{-1} s^{-1}. The total sample amount was 100 nmol and the sampling ratios (N_R) were 0.0204 (98:2), 1 (50:50) and 49 (2:98). The leading ion was chloride and the mobility was 79.08 · 10^{-5} cm^2 V^{-1} s^{-1}. The concentration of the leading ion was 10 mM and the migration current was 100 μA, which might be practical for a separation tube with I.D. = 0.5 mm. The pH of the leading electrolyte was 6 and the pH buffer was histidine (m_Q = 29.6 · 10^{-5} cm^2 V^{-1} s^{-1}). Apparently from Table II, the agreement between the exactly

TABLE I

PSYSICO-CHEMICAL CONSTANTS USED IN SIMULATION (25°C)

m_0 = Absolute mobility (10^{-5} cm^2 V^{-1} s^{-1}); pK_a = thermodynamic acid dissociation constants, assumed values being used for Cl$^-$, (SPADNS)$^-$ and (SPADNS)$^{2-}$.

Ion	m_0	pK_a
Cl$^-$	79.08	-2
(β-Alanine)$^+$	36.7	3.552
(Histidine)$^+$	29.7	6.04
(SPADNS)$^-$	21.0	-3
(SPADNS)$^{2-}$	42.0	-2
(SPADNS)$^{3-}$	63.0	3.55
(Monochloroacetate)$^-$	41.1	2.865
(Picrate)$^-$	31.5	0.708
(2,4-Dihydroxybenzoate)$^-$	32.0	3.395

TABLE II

EXACTLY SIMULATED RESOLUTION TIME (EXAC) AND APPROXIMATE RESOLUTION TIME (APPR) OF TWO-COMPONENT SYSTEM

n_A, n_B in nmol; m_A, m_B = absolute mobilities of components A and B (10^{-5} cm^2 V^{-1} s^{-1}); current = 100 μA; leading electrolyte, is 10 mM HCl–histidine (pH 6); approximate resolution time was evaluated using eqn. 3.

		Resolution time(s)								
		$n_A = 2$, $n_B = 98$			$n_A = 50$, $n_B = 50$			$n_A = 98$, $n_B = 2$		
m_A	m_B	EXAC	APPR	Difference (%)	EXAC	APPR	Difference (%)	EXAC	APPR	Difference (%)
60	59	8065	8551	6.0	8075	8573	6.2	8120	8642	6.4
60	58	3969	4229	6.6	4014	4250	5.9	4059	4320	6.4
60	57	2607	2788	6.9	2660	2810	5.6	2705	2879	6.4
60	56	1935	2068	6.9	1983	2089	5.3	2029	2158	6.4
60	55	1533	1635	6.7	1577	1657	5.1	1625	1726	6.2
60	50	719	771	7.2	765	792	3.5	810	862	6.4
30	29	5232	5658	8.1	5247	5655	7.8	5293	5747	8.6
30	28	2543	2783	9.4	2600	2779	6.9	2646	2871	8.5
30	27	1671	1824	9.2	1717	1821	6.1	1763	1913	8.5
30	26	1231	1345	9.3	1276	1342	5.2	1322	1434	8.5
30	25	964	1058	9.8	1011	1054	4.3	1057	1146	8.4
30	20	433	483	11.5	481	479	−0.4	528	571	8.1

evaluated and the approximated values is very good. It can be seen in Table II that the resolution time of the binary mixture was almost independent of the sampling ratio when the total sample amount was kept constant.

Table III shows the simulated potential gradient of the mixed zones (E_{AB}) for the same model mixtures as used in Table II. It is apparent that E_{AB} depends strongly on the sampling ratio. From this it is easily estimated that the mixed zone may be overlooked when a potential gradient or a conductivity detector is used. As shown for the actual samples in the next section, the situation is the same with UV detection.

Figs. 1 and 2 show the transient isotachopherograms of monochloroacetic acid and picric acid observed with the use of the array detector [8]. The ratios of the sample amounts (M:P) were 100:1, 20:1, 10:1, 5:1 and 2:1 in Fig. 1 and 1:1, 1:2, 1:5, 1:10 and 1:20 in Fig. 2. The total amount of the mixture injected was kept constant at 35 nmol. The boundaries between the leading and the MCA zones were rearranged at the same abscissa position. The small peak at the boundary was due to the small amount

of SPADNS added to the sample solution as a position marker. The zone distributions at the transient and steady states are apparent from Figs. 1 and 2. The mixed zone was distinguishable from both a UV-transparent monochloroacetic acid zone and a UV-absorbing picric acid zone, because the concentration of picric acid in the mixed zone was smaller than the separated steady-state zone when the concentration of picric acid in the sample is small. When the amount was increased, it became difficult to distinguish the mixed zone from the steady-state zone because the concentration of picric acid in the mixed zone was similar to that of the steady-state zone. The time-based zone lengths of the whole sample zones were almost constant during detection.

Fig. 3 summarizes the dependence of the resolution time on the ratio of the sample components. It is apparent that the resolution time of this mixture was almost constant and was independent of the ratio of sample components, although under the ultimate conditions the resolution of the mixed zone could not be observed clearly, as shown in Figs. 1 and 2.

TABLE III

SIMULATED POTENTIAL GRADIENT OF STEADY ZONES AND MIXED ZONES OF MODEL ANIONS

n_A, n_B in nmol; E_A, E_B and E_{AB} = potential gradients of steady zones A and B and that of the mixed zone AB, respectively; m_A, m_B = absolute mobilities of components A and B (10^{-5} cm^2 V^{-1} s^{-1}).

| m_A | m_B | Potential gradient (V cm^{-1}) | | | | |
| | | E_A | E_B | E_{AB} | | |
				$n_A = 2$, $n_B = 98$	$n_A = 50$, $n_B = 50$	$n_A = 98$, $n_B = 2$
60	59	69.5	70.8	70.8	70.2	69.6
60	58	69.5	72.0	72.0	70.8	69.6
60	57	69.5	73.4	73.3	71.4	69.6
60	56	69.5	74.7	74.6	72.1	69.7
60	55	69.5	76.1	76.0	72.7	69.7
60	50	69.5	84.1	83.8	76.4	69.8
30	29	143.8	149.1	149.0	146.5	144.0
30	28	143.8	154.8	154.6	149.2	144.1
30	27	143.8	160.9	160.5	152.1	144.2
30	26	143.8	167.5	167.0	155.2	144.3
30	25	143.8	174.6	174.0	158.5	144.4
30	20	143.8	221.9	220.0	179.0	145.1

On the other hand, the resolution time varies significantly when the charge of the sample component varies. This was investigated using a mixture of SPADNS and MCA. Fig. 4 shows the transient isotachopherogram observed for SPADNS and MCA. The ratio of the sample amounts (S:M) was 5:1, 2:1,

1:1, 1:2 and 1:5 and the total amount of the mixture injected was 50 nmol. The small peak at the boundary of the MCA and terminating zones was due to the small amount of picric acid used as a position marker.

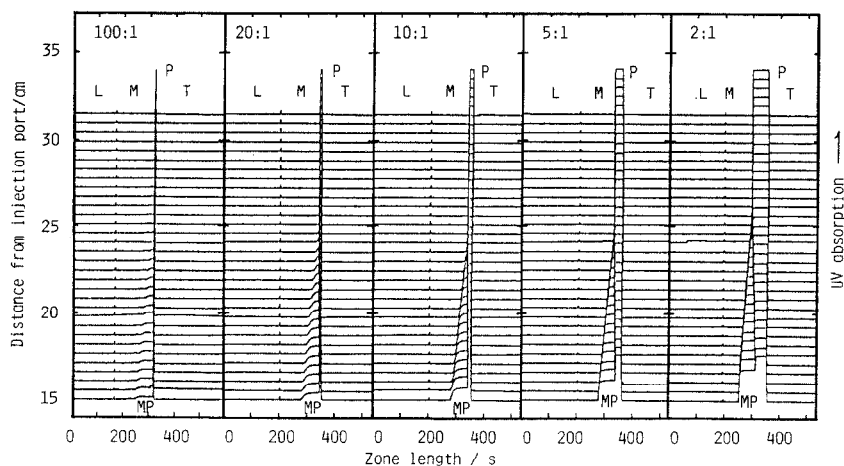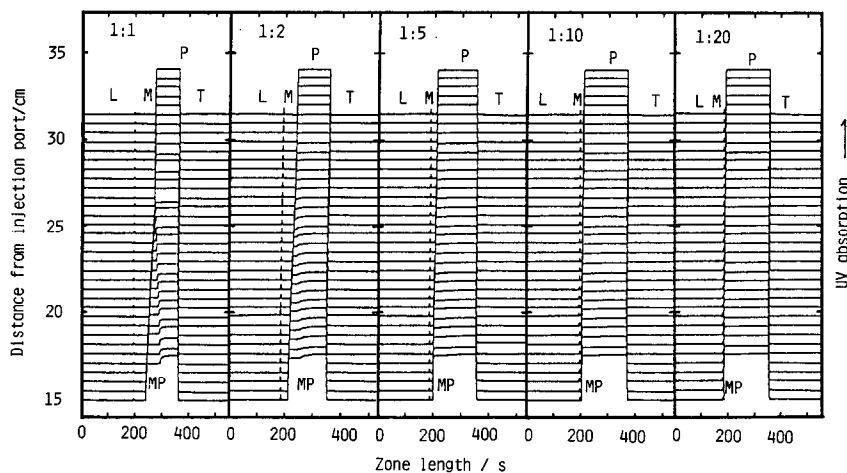Fig. 5 summarizes the dependence of the resolu-

Fig. 1. Transient isotachopherogram observed for monochloroacetic acid and picric acid by the use of a 32-channel UV array detector. The ratio of the sample amounts (M:P) was 100:1, 20:1, 10:1, 5:1 and 2:1. Total amount of the mixture injected, 35 nmol; pH of leading electrolyte, 3.6 (β-alanine buffer); migration current, 50 μA.

Fig. 2. Transient isotachopherogram observed for monochloroacetic acid and picric acid by the use of a 32-channel UV array detector. The ratio of the sample amounts (M:P) was 1:1, 1:2, 1:5, 1:10 and 1:20. Other conditions as in Fig. 1.

tion time on the ratio of the sample component. It is apparent that the resolution time of this system varies with the ratio of the sample components. As the zone length of SPADNS was about twice that for the same amount of MCA, the resolution time varied by a factor of two. As can be seen in Figs. 1, 2 and 4, it became difficult to distinguish the existence of the unresolved mixed zone only from an isotachopherogram if the sample had an extreme component ratio. The situation must be the same with potential gradient detection (PGD).
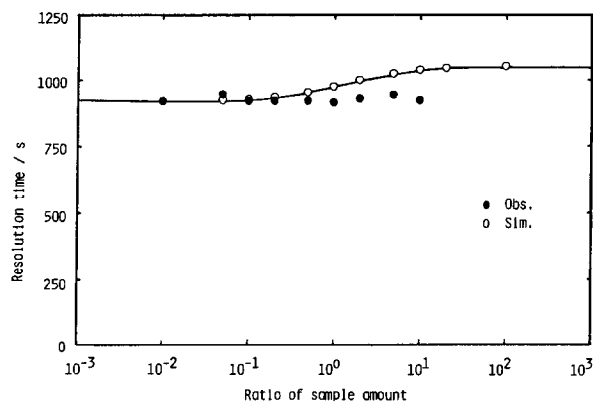
Fig. 3. Dependence of the resolution time on the ratio of the sample components. Samples, monochloroacetic acid and picric acid; total amount of the mixture injected, 35 nmol. Other conditions as in Fig. 1.

Fig. 6 shows the simulated isotachopherograms for equimolar and 10:1 MP. The total sample amount was 35 nmol and the migration current was $50\mu A$. Apparently from Fig. 6, the mixed zone of MP is distinguishable from the steady-state zones if the mixture is equimolar. However, the potential gradient of the mixed zone of the 10:1 mixture had a value very close to that of monochloroacetic acid.

Fig. 7 shows the actual isotachopherograms of MP (M:P = 10:1) obtained with PGD. The total sample amount injected was varied from 10 to 120 nmol. In Fig. 7, the two steps between picric acid and the terminator zones are due to the unknown impurities present in the electrolytes used. Apparently there was no mixed zone between monochloroacetic acid and picric acid, but in fact this was not so because, although the overall zone length increased linearly with the sample amount, as seen in Fig. 7, the increase in the minor component picric acid was not proportional to the increase in the total zone.

The observed zone length of monochloroacetic acid and picric acid is shown in Fig. 8. Apparently from Fig. 8, the relationship between the zone length of picric acid and the total sample amount injected had a bend at *ca.* 50 nmol, suggesting that the maximum sample load of the separation tube used was 50 nmol. When a total amount greater than 50 nmol was injected, the mixed zone of MP could not be resolved, although the mixed zone
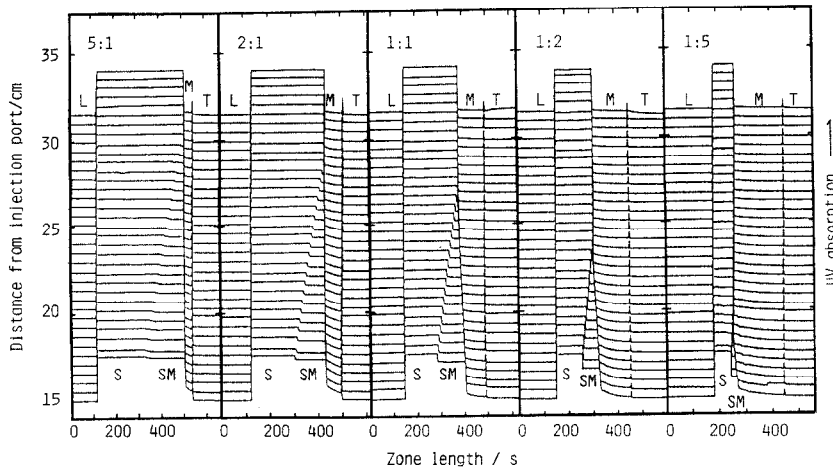
Fig. 4. Transient isotachopherogram observed for SPADNS and MCA. The ratio of the sample amounts (S:M) was 5:1, 2:1, 1:1, 1:2 and 1:5. Total amount of the mixture injected, 50 nmol; pH of leading electrolyte, 3.6 (β-alanine buffer); migration current, 50 μA.

could not be identified in Fig. 7 because the potential gradient of the mixed zone was almost the same as that of the monochloroacetic acid zone. Therefore, if one does not take account of such a bend, it is apparent that the minor component may be underestimated. The degree of underestimation depends, of course, on the amount of sample injected. If a larger amount is injected, a poorer accuracy will be obtained. In such a case, it is very important to measure zone lengths with varying sample amounts injected not only for the standard but also for the

actual sample. As discussed above, the overload can be easily found from the irregular behaviour of the zone length. Table IV summarizes the simulated concentrations, potential gradients and resolution times for the transient zone MP.

Multi-component mixture

The dependence of resolution time on the ratio of the sample amounts was simulated for a six-component system of model anions. The mobilities of model anions of A–F were 60 · 10^{-5}, 55 · 10^{-5}, 50 ·
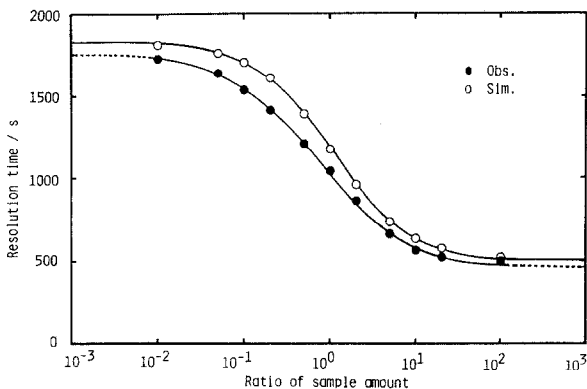

Fig. 5. Dependence of the resolution time on the ratio of the sample components. Samples, SPADNS and monochloroacetic acid. Total amount, 50 nmol. Other conditions as in Fig. 4.
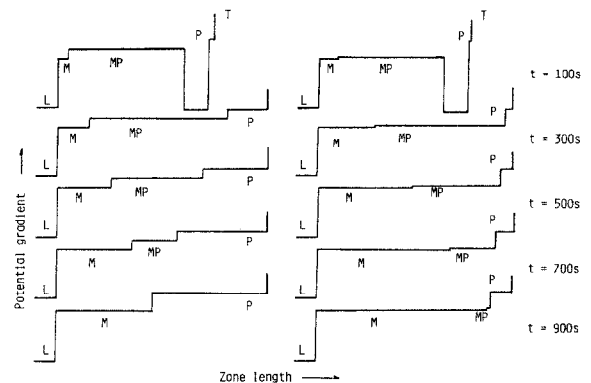

Fig. 6. Simulated isotachopherograms of equimolar and 10:1 mixtures of monochloroacetic acid and picric acid. Total sample amount, 35 nmol.
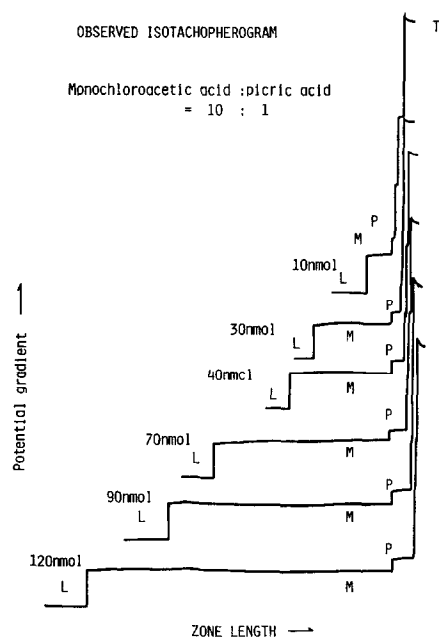
Fig. 7. Observed isotachopherograms of monochloroacetic acid (M)–picric (P) acid mixture (10:1) with the use of a potential gradient detector. Leading electrolyte (L), 5 mM HCl–β-alanine (pH 3.6); terminating electrolyte (T), 10 mM caproic acid; migration current, 50 μA.
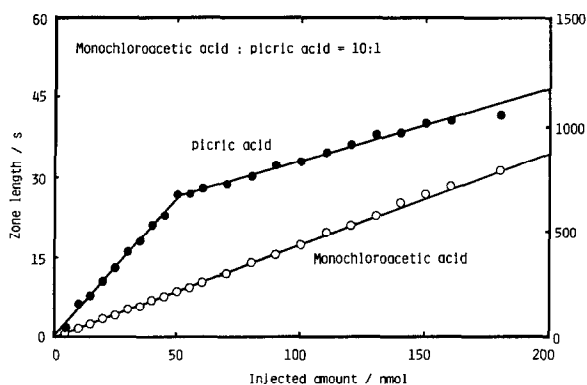

Fig. 8. Observed time-based zone length of monochloroacetic–picric acid mixture (10:1) vs. total molar amount. Conditions as in Fig. 7.

10^{-5}, $45 \cdot 10^{-5}$, $40 \cdot 10^{-5}$ and $35 \cdot 10^{-5}$ cm^2 V^{-1}s^{-1}. The pK_a values are assumed to be -1. The total amount of the components was kept constant at 100 nmol and the amount of component A was increased and the others were decreased.

Fig. 9 shows the separation diagram for the six model anions for equimolar, 4:1:1:1:1:1 and 8:1:1:1:1:1 mixtures. The leading ion was 10 mM chloride and the pH of the leading electrolyte was 6 (histidine buffer). The migration current was 100

TABLE IV

SIMULATED CONCENTRATIONS, POTENTIAL GRADIENTS AND RESOLUTION TIMES FOR THE TRANSIENT ZONES OF MONOCHLOROACETIC ACID AND PICRIC ACID

Total sample amount, 35 nmol; leading electrolyte, 5 mM HCl–β-alanine (pH 3.6); migration current, 50 μA. $C_{t,M,MP}$ and $C_{t,P,MP}$ = total concentration (mM) of monochloroacetic acid and picric acid in the transient mixed zone; E_{MP} = potential gradient (V cm^{-1}) of the mixed zone. Steady state: $C_{t,M}$ = 3.67 mM, $C_{t,P}$ = 3.10 mM, E_M = 86.8 V cm^{-1} and E_P = 103.8 V cm^{-1}.

| | Monochloroacetic acid (M) : picric acid (P) | | | | | | | | |
	100:1	10:1	5:1	2:1	1:1	1:2	1:5	1:10	1:100
t_A	151.1	138.7	127.2	101.7	76.30	50.86	25.43	13.87	1.511
t_B	1.790	16.44	30.14	60.27	90.41	120.5	150.7	164.4	179.0
pH$_M$	3.820	3.822	3.824	3.827	3.831	3.834	3.837	3.838	3.840
$C_{t,M,MP}$	3.621	3.234	2.890	2.185	1.549	0.976	0.462	0.245	0.026
$C_{t,P,MP}$	0.041	0.366	0.657	1.252	1.788	2.272	2.706	2.889	3.074
E_{MP}	87.03	88.53	89.92	92.91	95.81	98.61	101.3	102.5	103.7
$v_{M/MP}$	2.559	2.604	2.645	2.735	2.821	2.905	2.984	3.019	3.056
m_M	35.24	35.26	35.28	35.32	35.35	35.39	35.42	35.43	35.45
m_P	29.41	29.41	29.42	29.43	29.45	29.46	29.47	29.47	29.47
$t_{res,MP}$	923.0	930.5	938.1	956.3	977.0	1000	1026	1039	1054
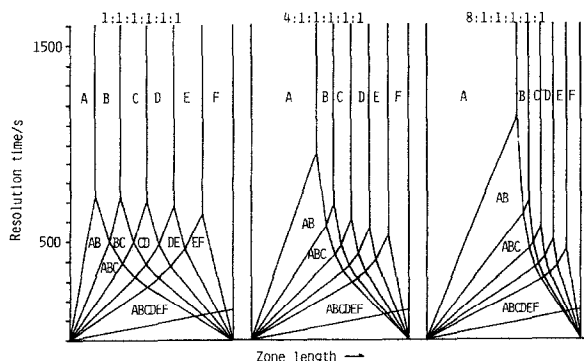
Fig. 9. Separation diagrams simulated for an equimolar six-component mixture of model anions (A–F). The mobilities of A–F were $60 \cdot 10^{-5}$, $55 \cdot 10^{-5}$, $50 \cdot 10^{-5}$, $45 \cdot 10^{-5}$, $40 \cdot 10^{-5}$ and $35 \cdot 10^{-5}$ cm^2 V^{-1} s^{-1}, respectively. The pK_a values were assumed to be -1. The total amount of separands was 100 nmol. For the equimolar mixture, the amount of A–F was 16.67 nmol, for the 4:1:1:1:1:1 mixture the amount of A was 44.44 nmol and that of B–F was 11.11 nmol and for the 8:1:1:1:1:1 mixture, the amount of A was 61.54 and that of B–F was 7.69 nmol.
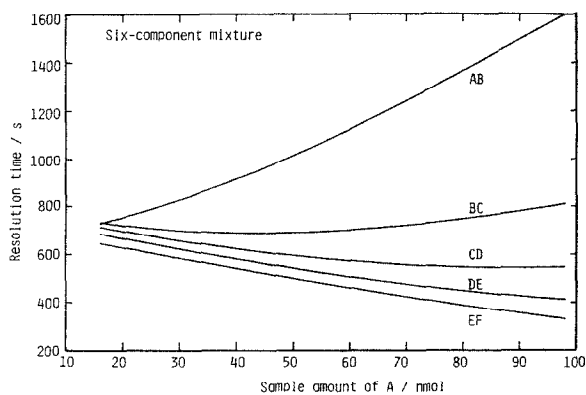

Fig. 10. Amount of component A *vs.* resolution time of the mixed zones AB, BC, CD, DE and EF for a six-component model mixture (total amount = 100 nmol). Simulation conditions as in Fig. 9. The migration current was 100 μA.

The amount of A was 75 nmol and S was 0.056. In this instance the difference in $t_{res,AB}$ was very small because of the coexisting components of A and B,

μA. The amount of B–F in the equimolar mixture is twice that in the 8:1:1:1:1:1 mixture. If the components E and F are separated independently as a binary mixture, the resolution time of equivalent amounts of E and F in these cases should differ by a factor of two. However, as seen in Fig. 9, the resolution time of E and F for the 8:1:1:1:1:1 mixture slightly smaller than that for the equimolar mixture. This can be explained by the effect of the coexisting components being more significant with the 8:1:1:1:1:1 mixture than with the equimolar mixture.

Fig. 10 shows the simulated dependence on the ratio of the components of the resolution time for five binary mixed zones of a six-component mixture. Apparently, $t_{res,AB}$ increased with increase in the total amount of A and B. The resolution time of the other mixed zones (BC, CD, DE and EF) decreased gradually with increase in the amount of A. The $t_{res,AB}$ value for the six-component equimolar mixture [$t_{res,AB}(6)$] was 733.5 s [16.67 nmol each, separation number [5,6] (S) = 0.22] and that of the binary mixture [$t_{res,AB}(2)$] was 526.0 s (S = 0.031). The difference was caused by the effect of the coexisting components on the potential gradient of the mixed zone AB. With the 15:1:1:1:1:1 mixture, $t_{res,AB}(6)$ was 1303.3 s and $t_{res,AB}(2)$ was 1294.7 s.
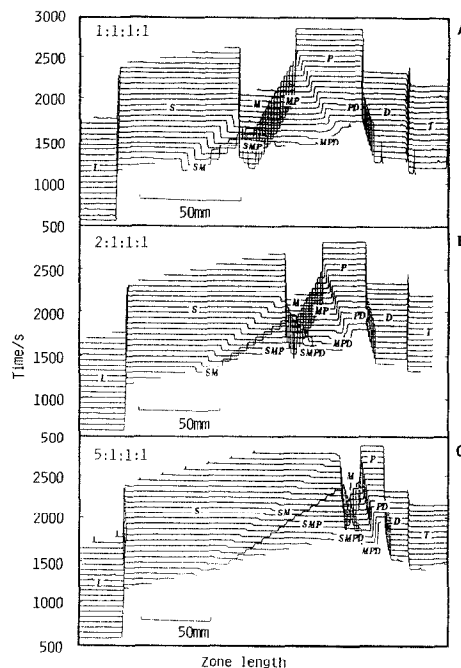

Fig. 11. Observed separation process for a mixture of SPADNS, monochloroacetic acid, picric acid and 2,4-dihydroxybenzoic acid with the use of a scanning UV detector. The ratio of the component amounts was (A) 1:1:1:1, (B) 2:1:1:1 and (C) 5:1:1:1. Leading electrolyte, 5 mM HCl–β-alanine (pH 3.6); terminating electrolyte, 10 mM caproic acid; migration current, 50 μA.

i.e., the amount of C–F is smaller than for the equimolar mixture. On the other hand, for example, $t_{res,EF}(6)$ was 642.3 s for the six-component equimolar mixture and $t_{res,EF}(2)$ was 400.3 s ($S = 0.0250$ and 0.04018, respectively). With the 15:1:1:1:1:1 mixture, the amount of B–F was 5 nmol. The $t_{res,EF}(6)$ value was 404.5 s and $t_{res,EF}(2)$ was 120.2 s ($S = 0.012$ and 0.040, respectively). The significant delay was due to the large amount of the coexisting ions A–D (total amount $= 90$ nmol). From this simulation it is concluded that the resolution time of a sample present in a very small amount in a matrix is affected by the coexistence of the other components. If the total amount of the mixture is kept constant, it depends on the ratio of the sample amount, although the dependence is not very strong.

This effect was observed for the mixture of SPADNS, monochloroacetic acid, picric acid and 2,4-dihydroxybenzoic acid. The total amount was 100 nmol and the ratio was varied as 1:1:1:1, 2:1:1:1, 5:1:1:1 and 10:1:1:1. The leading electrolyte was 5.00 mM hydrochloric acid–β-alanine (pH 3.6) and the migration current was 50 μA. Fig. 11 shows the transient isotachopherograms obtained with the use of the scanning UV detector [4] except for the 10:1:1:1 case. Table V and Fig. 12 summarize the observed resolution times of the mixed zones. Good agreement was obtained, confirming our theoretical estimates.

From Fig. 11 and Table V, it is apparent that the resolution time of the mixed zone of SPADNS and monochloroacetic acid (SM) increased with increase in SPADNS concentration, the values being 1199, 1526, 2118 and 2472 s, respectively. On the other hand, the resolution time of picric acid and

TABLE V

RESOLUTION TIME OF MIXED ZONE IN THE SEPARATION PROCESS OF SPADNS, MONOCHLOROACETIC ACID, PICRIC ACID AND 2,4-DIHYDROXYBENZOIC ACID

Total amount $= 100$ nmol; leading electrolyte, 5 mM HCl–β-alanine (pH $= 3.6$); migration current, 50 μA. S:M:P:D $=$ SPADNS : monochloroacetic acid : picric acid : 2,4-dihydroxybenzoic acid.

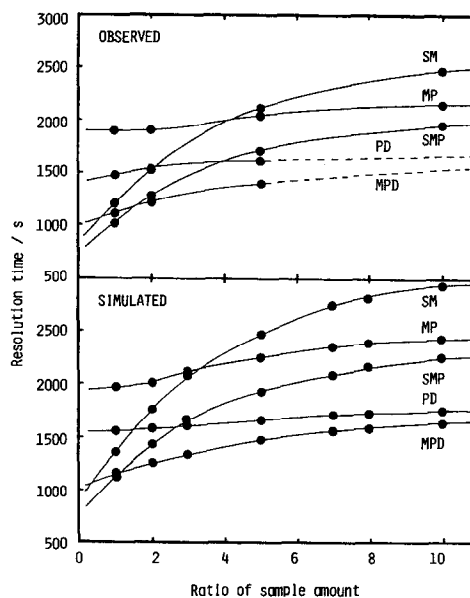| S:M:P:D	Mixed zones	Resolution time(s)		
		Observed	Simulated	Difference (%)
1:1:1:1	SM	1199	1306	8.9
	MP	1896	1915	1.0
	PD	1469	1514	3.1
	SMP	1014	1075	6.0
	MPD	1110	1154	4.0
	SMPD	–	823	–
2:1:1:1	SM	1526	1737	13.8
	MP	1908	1968	3.1
	PD	1548	1547	−0.1
	SMP	1279	1387	8.4
	MPD	1220	1251	2.5
	SMPD	–	1034	–
5:1:1:1	SM	2118	2445	15.4
	MP	2049	2171	6.0
	PD	1614	1648	2.1
	SMP	1715	1870	9.0
	MPD	1401	1459	4.1
	SMPD	1275	1353	6.1
10:1:1:1	SM	2472	2919	18.1
	MP	2150	2352	9.4
	PD	–	1730	–
	SMP	1955	2183	11.7
	MPD	–	1614	–
	SMPD	1420	1556	9.6

Fig. 12. Observed and simulated resolution times of four-component mixture of SPADNS (S), monochloroacetic acid (M), picric acid (P) and 2,4-dihydroxybenzoic acid (D). The abscissa scale corresponds to S:M:P:D $= 1:1:1:1$ to $10:1:1:1$. Conditions as in Fig. 11.

2,4-dihydroxybenzoic acid (PD) increased slightly (1469, 1548 and 1614 s). This increase was not simulated for the model strong electrolytes. The cause of the difference between the simulation for strong electrolytes and the observation for the present sample was due to the fact that 2,4-dihydroxybenzoic acid is a weak electrolyte and the difference in the pH of the mixed zones affected the resolution time. Although we emphasized resolution time under a constant migration current from a practical viewpoint, it should be noted that the essential factor is the amount of electricity applied during the migration process [1,2].

In conclusion, the present simulation and experiments confirmed that isotachophoresis has very high separation efficiency even for the separation of minor components in a matrix. If a highly sensitive detection method could be applied, the utility of isotachophoresis would be increased. We are currently trying to use particle-induced X-ray emission (PIXE) for the targets fractionated off-line.

REFERENCES

1 P. Bocek, M. Deml, B. Kaplanova and J. Janak, J. Chromatogr., 160 (1978) 1.
2 P. Gebauer and P. Bocek, J. Chromatogr., 320 (1985) 49.
3 T. Hirokawa, Y. Yokota and Y. Kiso, J. Chromatogr., 545 (1991) 267.
4 T. Hirokawa, Y. Yokota and Y. Kiso, J. Chromatogr., 538 (1991) 403.
5 F. E. P. Mikkers, F. M. Everaerts and J. A. F. Peek, J. Chromatogr., 168 (1979) 293.
6 F. E. P. Mikkers, F. M. Everaerts and J. A. F. Peek, J. Chromatogr., 168 (1979) 317.
7 G. Brouwer and G. A. Postema, J. Electrochem. Soc., 117 (1970) 874.
8 T. Hirokawa, K. Nakahara and Y. Kiso, J. Chromatogr., 463 (1989) 39.
9 T. Hirokawa, K. Nakahara and Y. Kiso, J. Chromatogr., 463 (1989) 51.
10 T. Hirokawa, K. Nakahara and Y. Kiso, J. Chromatogr., 470 (1989) 21.